Supporting Information

High–Performance Visible–Light–Driven Plasmonic Photocatalysts Ag/AgCl with Controlled Size and Shape using Graphene Oxide as Capping Agent and Catalyst Promoter

Mingshan Zhu,[†] *Penglei Chen,*[†,‡,*] *and Minghua Liu*[†,*]

[†]Beijing National Laboratory for Molecular Science, CAS Key Laboratory of Colloid, Interface and Chemical Thermodynamics, Institute of Chemistry, Chinese Academy of Sciences, No. 2 Zhongguancun Beiyijie, Beijing 100190, P. R. China. [‡]College of Chemistry and Molecular Engineering, Zhengzhou University, 100 Science Road, Zhengzhou, Henan 450001, P. R. China.

E–mail: chenpl@iccas.ac.cn, cpl@zzu.edu.cn (P.C.); liumh@iccas.ac.cn (M.L.)

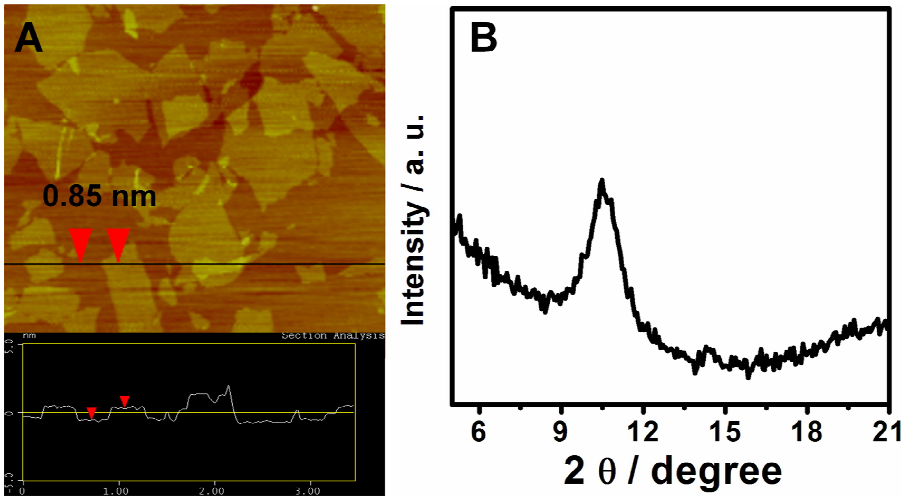

Figure S1. A: AFM image (A) and XRD pattern (B) of our GO nanosheets.

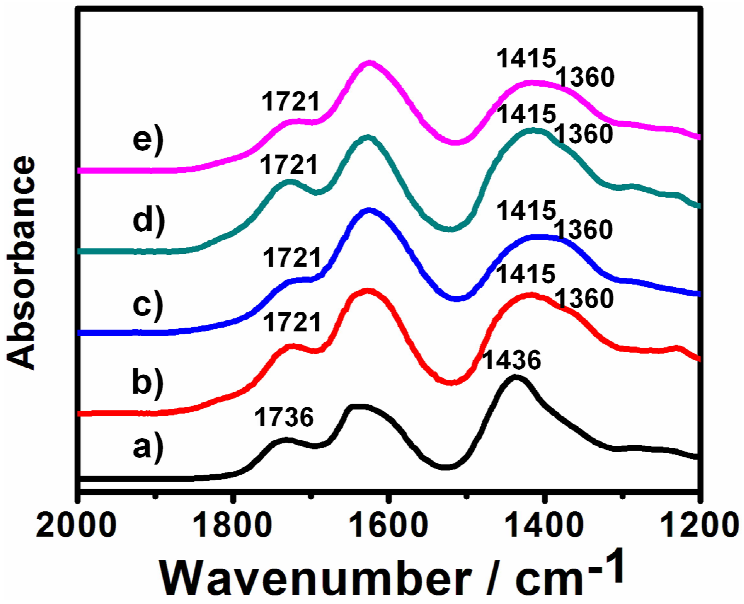

Figure S2. FT–IR spectra of our original powdery GO (a), and those of the near–spherical (b and c) and cube–like (d and e) Ag/AgCl/GO fabricated in the $AgNO_3$ (b and d) and $Ag(NH_3)_2NO_3$ (c and e) systems.

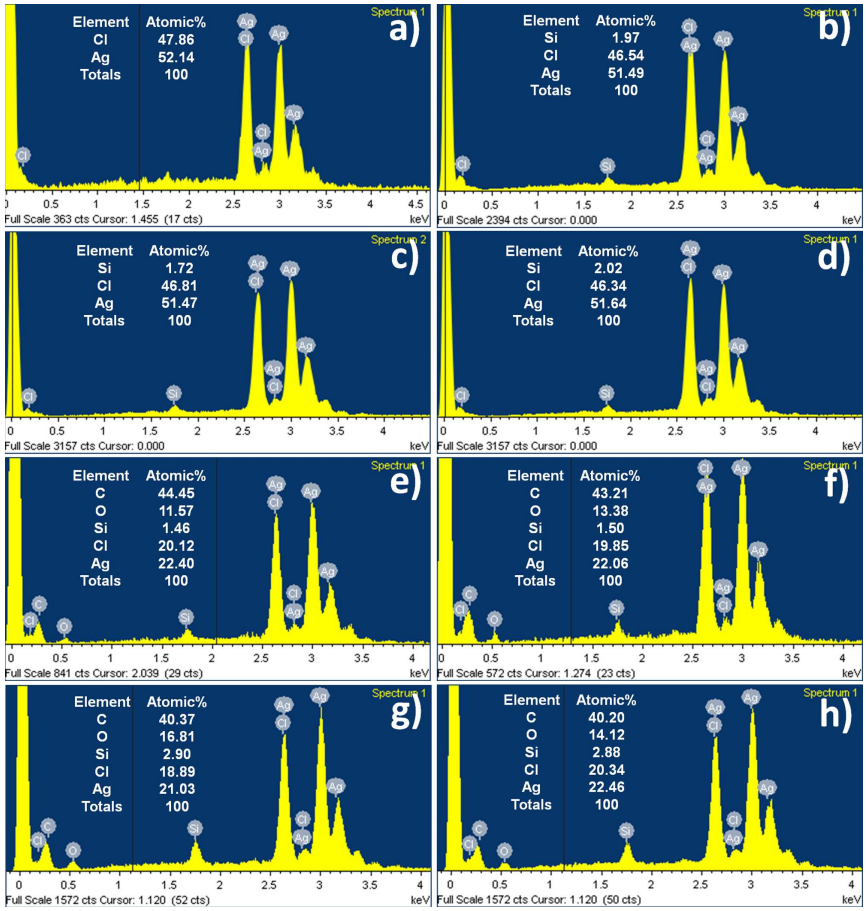

Figure S3. EDX elemental analysis of the Ag/AgCl (a–d) and Ag/AgCl/GO (e–h) fabricated in $AgNO_3$ (a, c, e and g) and $Ag(NH_3)_2NO_3$ (b, d, f and h) systems at 0 °C (a, b, e and f) and 30°C (c, d, g and h). The quantitative elemental analysis results for each sample are listed in the corresponding panels. The signals ascribing to Si element could also be detected, since Si plates were used as the solid support for the measurement.

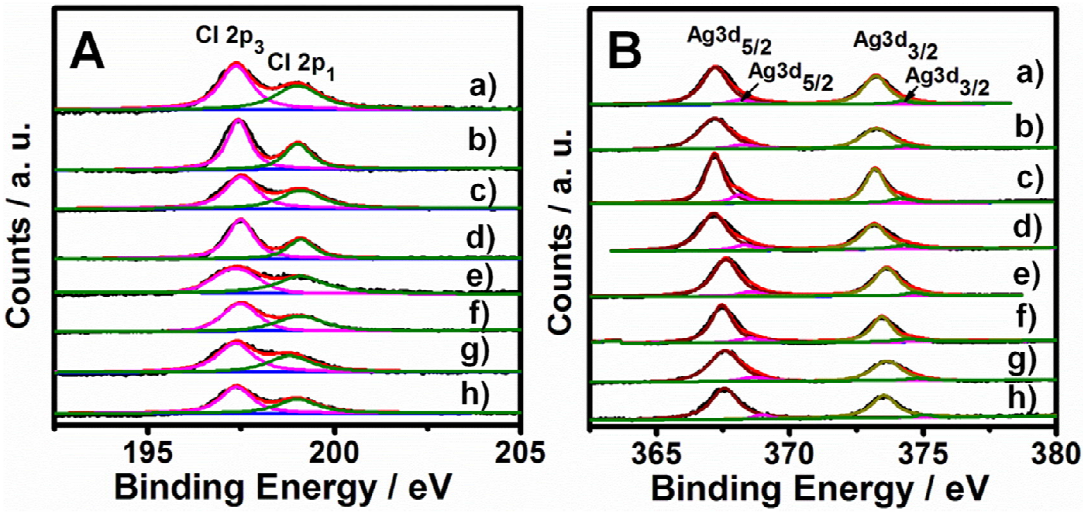

Figure S4. XPS spectra of Cl 2p (A) and Ag 3d (B) of Ag/AgCl (a–d) and Ag/AgCl/GO (e–h) nanostructures fabricated in $AgNO_3$ (a, c, e and g) and $Ag(NH_3)_2NO_3$ (b, d, f and h) systems at 0 °C (a, b, e and f) and 30°C (c, d, g and h).

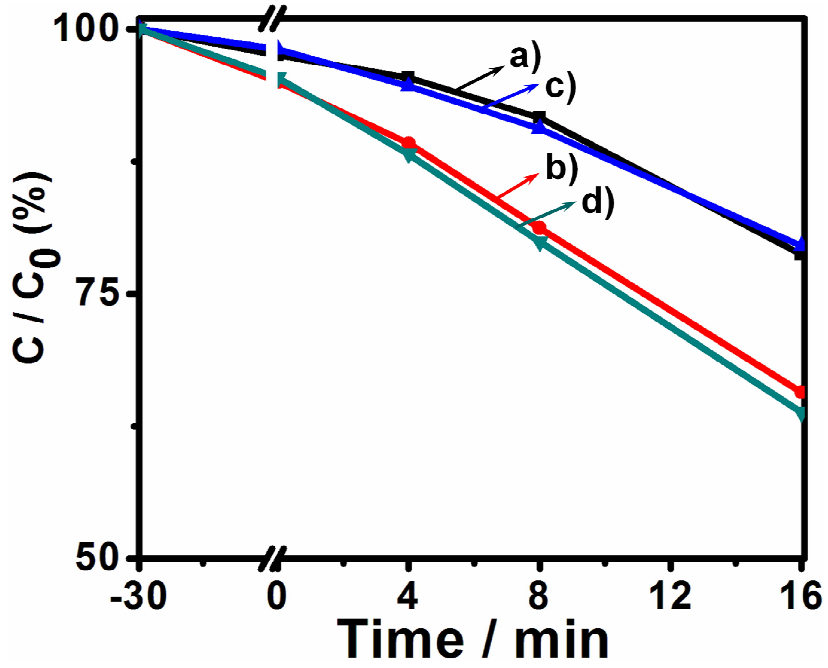

Figure S5. Photocatalytic activities of the Ag/AgCl-500 NS (a) and Ag/AgCl-500 NC (b) fabricated in $AgNO_3$ systems, those of the Ag/AgCl-500 NS (c) and Ag/AgCl-500 NC (d) fabricated in $Ag(NH_3)_2NO_3$ systems are also presented for comparison.

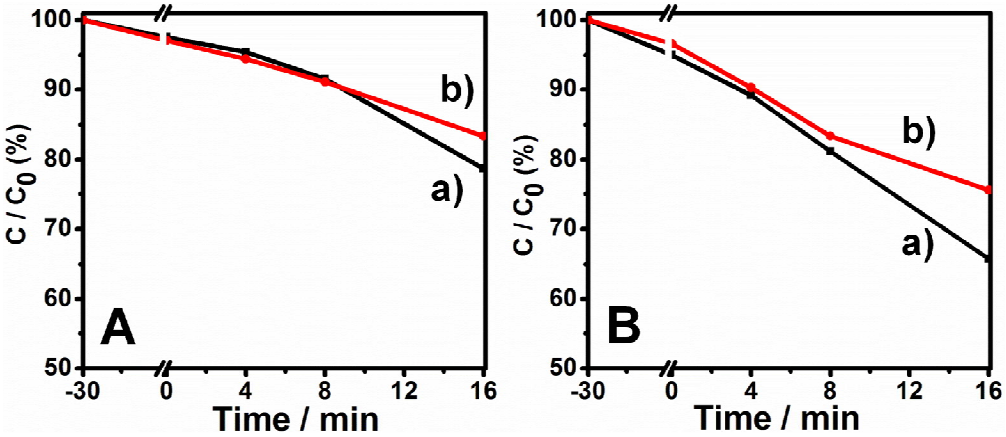

Figure S6. Catalytic activities of the bare Ag/AgCl-500 NS (A, curve a) and Ag/AgCl-500 NC (B, curve b) for the degradation of MO pollutants under visible light irradiation. Those of the mixture of bare Ag/AgCl and GO are also presented (curve b) in the corresponding panel for comparison.

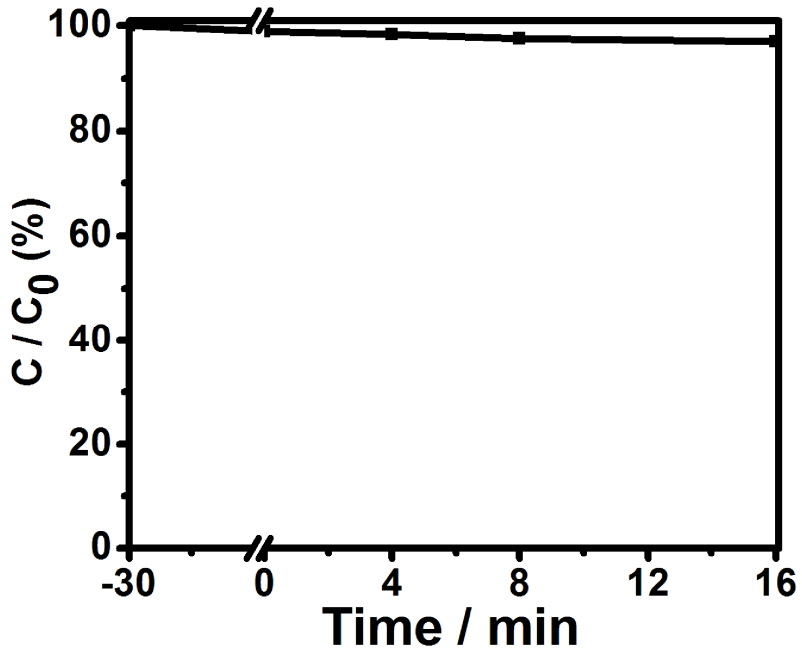

Figure S7. Catalytic activities of our GO for the degradation of MO pollutants under visible light irradiation.

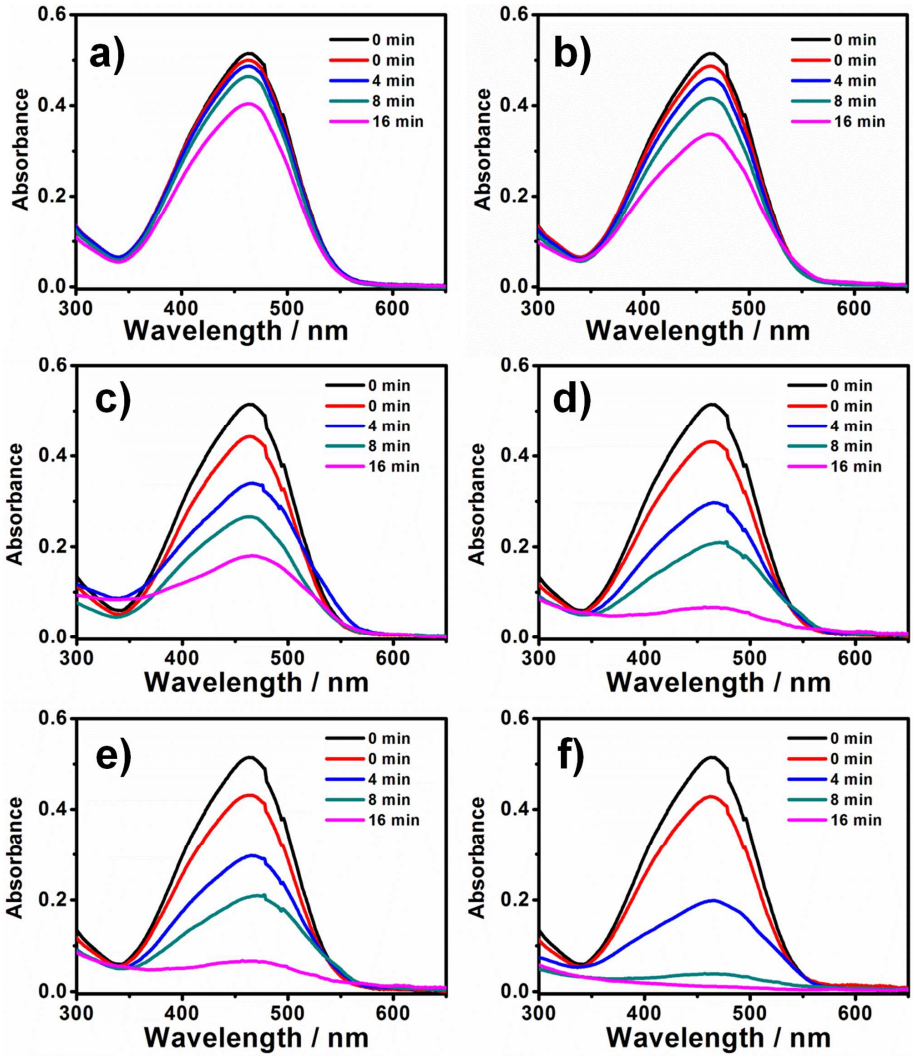

Figure S8. Typical real–time absorption spectra of MO dye during the photodegradation process over (a) Ag/AgCl–500 NS, (b) Ag/AgCl–500 NC, (c) Ag/AgCl/GO–200 NS, (d) Ag/AgCl/GO–100 NS, (e) Ag/AgCl/GO–200 NC, (f) Ag/AgCl/GO–100 NC nanostructures under visible–light irradiations. The black and red curves marked as 0 min in each panel are the absorption spectra detected from the original MO solution before (black) and after (red) the dark adsorption experiment, respectively.

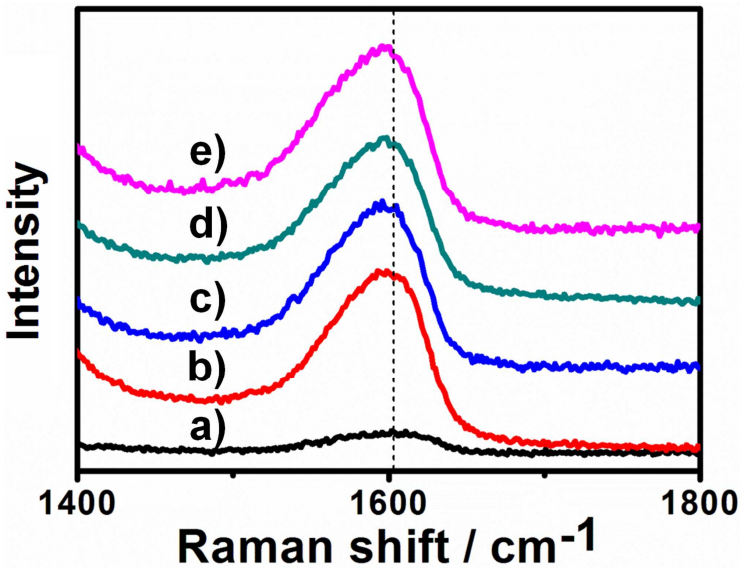

Figure S9. Raman spectra of our original powdery GO (a) and the Ag/AgCl/GO nanostructures: Ag/AgCl/GO–100 NS (b), Ag/AgCl/GO–200 NS (c), Ag/AgCl/GO–100 NC (d) and Ag/AgCl/GO–200 NC (e).

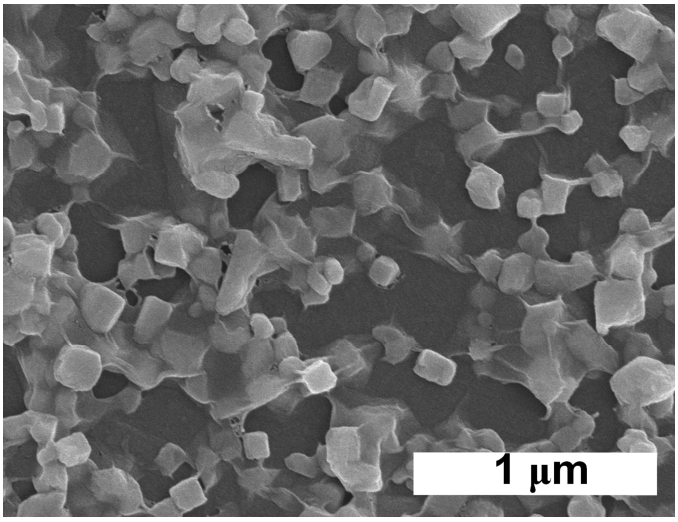

Figure S10. Typical SEM image of the Ag/AgCl/GO–100 NC nanostructures after the photocatalytic degradation of MO dye under visible–light irradiation.

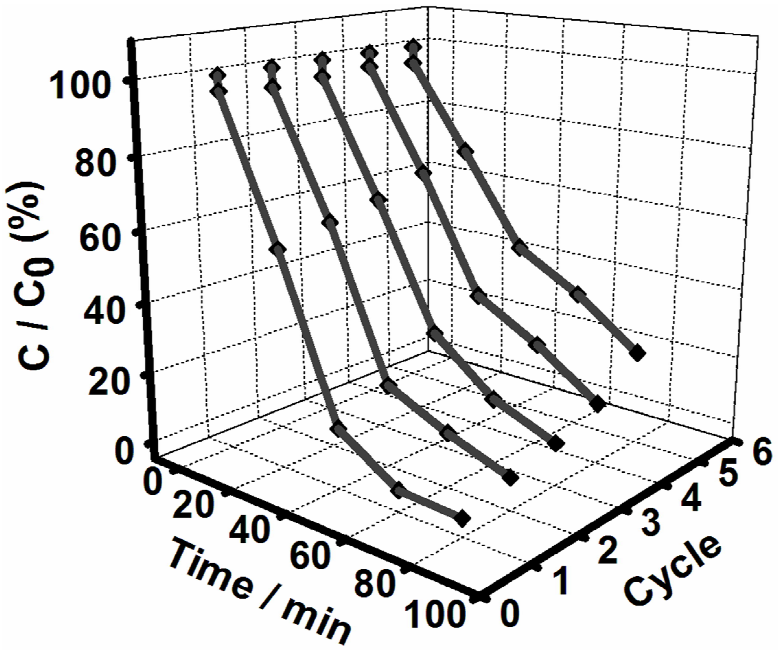

Figure S11. Five consecutive cycling photodegradation curves of MO pollutant over our Ag/AgCl-500 NC photocatalysts under visible light irradiation.

Supporting Discussions on XPS and Raman Spectra:

Besides the experimental facts deduced from the EIS of the main context (Figure 7), the XPS (Figure S4B) and Raman spectra (Figure S9) of our samples were also investigated to further verify the occurrence of charge transfer between Ag/AgCl and GO in our GO–hybridized nanocomposites. As shown in Figure S4B, when GO nanosheets are not involved in the synthesis systems, the XPS spectra of the samples (namely, the bare Ag/AgCl nanospecies) formulated both in the $AgNO_3$ and $Ag(NH_3)_2NO_3$ systems display a binding energy of Ag $3d_{5/2}$ and Ag $3d_{3/2}$ at about 367.1 and 373.2 eV, respectively.[S1, S2] Four bands at *ca.* 367.1, 368.1 eV and 373.2, 374.1 eV could be deduced *via* a deconvolution of these two bands, respectively.[S1, S2] In contrast, in the cases of the Ag/AgCl/GO nanocomposites formulated with the presence of GO nanosheets, all the peaks of Ag $3d_{5/2}$ and Ag $3d_{3/2}$ shift to a higher binding energy by *ca.* 0.5 eV compared with the bare Ag/AgCl nanostructures. These facts further suggest that the Ag/AgCl species in our Ag/AgCl/GO nanocomposites serve as electron–donor component, while GO work as electron–acceptor.[S1–S3]

On the other hand, it has been proved that the occurrence of charge transfer between GO and the hybridized components could also be verified by the Raman spectra, wherein it has

been demonstrated that the *G*–band of GO nanosheets shifts to lower frequency when GO is hybridized with an electron–donor component, while it shifts to higher frequency when an electron–acceptor component is hybridized.[S1, S4–S6] As shown in Figure S9, a *G* –band at *ca.* 1602 cm^{-1}, which is a typical Raman feature of GO nanosheets, could be observed from our original powdery GO species. In contrast, the *G*–band shifts by 6 cm^{-1} to a lower frequency at 1596 cm^{-1} for the Ag/AgCl/GO nanocomposites. Together with the results from EIS (Figure 7) and XPS (Figure S4B), these facts further verifies the occurrence of charge transfer between Ag/AgCl and GO of our GO–hybridized nanocomposites, wherein Ag/AgCl and GO species work as electron–donor and electron–acceptor components, respectively.

Supporting References:

S1 Zhu, M.; Chen, P.; Liu, M. *ACS Nano* **2011**, *5*, 4529–4536.

S2 Zhu, M.; Chen, P.; Liu, M. *J. Mater. Chem.* **2011**, *21*, 16413–16419.

S3 D. Briggs, Handbook of X–ray and Ultraviolet Photoelectron Spectroscopy, Heyden, London, **1977**.

S4 Xu, Y.; Wu, Q.; Sun, Y.; Bai, H.; Shi, G. *ACS Nano* **2010**, *4*, 7358–7362.

S5 Ghosh, A.; Rao, K. V.; George, S. J.; Rao, C. N. R. *Chem. Eur. J.* **2010**, *16*, 2700–2704.

S6 Das, A.; Pisana, S.; Chakraborty, B.; Piscanec, S.; Saha, S. K.; Waghmare, U. V.; Novoselov, K. S.; Krishnamurthy, H. R.; Geim, A. K.; Ferrari, A. C.; Sood, A. K. *Nat. Nanotechnol.* **2008**, *3*, 210–215.